ORNL/SPR-2020/1672

Technology Enabling Zero-EPZ Micro Modular Reactors

Milestone M2.2.2

Fabrication of Zirconium Hydride with Controlled Hydrogen Loading

Principal Investigator: Jason R. Trelewicz
Award Number: DE-AR0000977
Prime Recipient: Stony Brook University
Sub-recipients: University of Tennessee Knoxville Oak Ridge National Laboratory
Project Period: 03/13/2019 – 09/12/2021
Milestone report #: 2.2.2
Milestone authors: Xunxiang Hu (ORNL) Peter Mouche (ORNL) Danny Schappel (ORNL) David Sprouster (SBU)
Due date: 09/12/2020
Report submission date: 09/12/2020

SUMMARY

This report completes Milestone M2.2.2 - ZrH pellet fabricated with controlled hydride loading: ZrH1.5±0.1 single phase pellets fabricated with controlled and thermally stable hydride loading. Hydrogen content to be quantified and single-phase confirmed by X-ray diffraction. In this milestone, we report the successful fabrication of delta-phase zirconium hydride pellets using the ORNL bulk metal hydriding system. The successful deployment of zirconium hydride moderator in advanced reactors requires development of a consistent and affordable production pathway along with implementation of a hydrogen retention solution throughout the reactor life. Fabrication of delta-phase zirconium hydride is challenging since the absorption of a large amount of hydrogen into alpha-zirconium induces significant volume expansion and the present hydrogen concentration gradient results in cracking. A fully programmable hydriding system with continuous hydrogen partial pressure and flow control to facilitate processing of massive metal hydride has been developed at ORNL. In this report, the working principle of the hydriding system will be introduced. Characterization of the produced zirconium hydride includes X-ray powder diffraction to identify the present phases and X-ray Computed Tomography to visualize the internal microstructure (including cracks). The results indicate that single delta-phase zirconium hydride pellets with various sizes have been successfully produced.

CONTENTS

FIGURES

TABLES

ACRONYMS

ARPA-E	Advanced Research Projects Agency-Energy
BCC	Body-centered cubic
EBW	Electron beam welding
FCC	Face-centered cubic
H	Hydrogen
HCP	Hexagonal closest packed
MEITNER	Modeling-Enhanced Innovations Trailblazing Nuclear Energy Reinvigoration
ORNL	Oak Ridge National Laboratory
SNAP	Systems Nuclear Auxiliary Power
TCR	Transformational Challenge Reactor
TRIGA	Training, Research, Isotopes, General Atomic research reactors
XCT	X-ray computed tomography
XRD	X-ray diffraction
Zr	Zirconium
ZrH_x	Zirconium hydride

ACKNOWLEDGMENTS

The authors appreciate the support of the Advanced Research Projects Agency-Energy (ARPA-E) program: Modeling-Enhanced Innovations Trailblazing Nuclear Energy Reinvigoration (MEITNER) under contract DE-AR0000977.

1 INTRODUCTION

Hydrogen has broad applications in both nuclear and non-nuclear systems [1]. Hydrogen is an outstanding moderator for neutrons of less than a few MeV of kinetic energies in nuclear systems by reason of its substantial equivalence in mass to the neutron, its low neutron absorption cross section, and its acceptably high neutron scattering cross section. This characteristic is useful for slowing down fission neutrons to a level at which they have a greater probability of interacting with other fissile, fertile, and neutron-control atoms. Given its high energy density, hydrogen itself is also an ideal energy carrier, averts adverse effects on environment, and reduces dependence on imported oil for countries without natural resources. Hydrogen storage is clearly a key enabling technology for the development of a hydrogen economy [2]. Metal hydrides have been perceived as an efficient, low-risk option for high-density hydrogen storage since the late 1970s. Transition metals are known to absorb large quantities of hydrogen to form metal-hydrogen solid solution at low hydrogen content and the hydride compounds at higher hydrogen content. The atomic density of hydrogen in many of these materials is far greater than in liquid hydrogen itself.

Metal hydrides are particularly well suited to thermal reactor system in which core weight and volume need to be minimized, where they serve as a constituent in fuels and in moderator and shield materials. Table 1 shows the basic properties of selected metal hydrides that have potential application in nuclear systems [3]. It is apparent that zirconium hydride (ZrH_x) is the most promising moderator material in terms of the moderating ratio (the ratio of the macroscopic slowing-down power to the macroscopic cross section for neutron absorption). It has been frequently used as a high-performance moderating material in advanced reactors. Examples include the Systems Nuclear Auxiliary Power (SNAP) Program [4]; Training, Research, Isotopes, General Atomic (TRIGA) research reactors [5]; and nuclear thermal propulsion reactors [6]. In these cases, ZrH_x is purposefully used as the matrix for fissile materials in nuclear fuel applications. The most common type of hydride fuel consists of metallic uranium dispersed in a ZrH_x matrix with a nominal composition of U(30wt%)-$ZrH_{1.6}$. Higher power density, high moderator density inherent to the fuel, large prompt negative fuel-temperature reactivity feedback, and higher thermal conductivity are attractive attributes of this class of fuels [5].

Table 1. Properties of metal hydrides having potential nuclear application [3]

Hydride	Attainable hydrogen density		Hydride density (g/cm^3)	Slowing down power	Moderating ratio
	10^{22}atoms H/cm^3	g H/cm^3			
TiH_2	9.1	0.152	3.78	1.85	6.3
ZrH_2	7.3	0.122	5.56	1.45	55
LiH	5.8	0.095	0.78	1.2	3.5
YH_2	5.8	0.097	4.24	1.2	25
ThH_2	4.9	0.082	9.5	1.0	5.2
H_2O	6.6	0.110	0.98	1.35	70
$ThZr_2H_7$	7.7	0.129	7.75	1.55	14
$ThTi_2H_6$	8.8	0.147	8.15	1.8	6

There is a need for thermally and chemically stable massive metal hydrides for use in shield, reflector, moderator, and moderator-fuel in nuclear reactor components. The common method of preparing metal hydrides is by direct reaction of the metal with hydrogen, guided by the phase diagram and the pressure-composition-temperature relationship. The reaction of hydrogen with the metals (e.g, Zr, Y, Ti, Th) is a diffusion-controlled exothermic process that normally results in expansion of the metal lattice as the hydrogen enters portions of the lattice. This gives rise to a substantial decrease in density and represents a significant volume expansion during the hydriding process (e.g., 19% in the case of TiH_2, 14.3% in the case of ZrH_2, 6% in the case of YH_2). Such changes produce severe stresses in the massive metal hydrides since the diffusive nature of the hydriding process results in a large hydrogen concentration gradient from the surface to core of a material. During the hydriding process, a hydride case forms near the surface, while hydrogen in the interior of the specimen is dispersed (i.e., a solid solution). The material growth accompanying hydride formation, namely at the interface between the hydride case and the interior, generates stresses that can easily exceed the fracture strength of the hydride and cause extensive cracking. Therefore, to prepare massive monolithic forms of metal hydride, this cracking must be avoided—which is challenging [7] [8].

In this report, we summarize our efforts to fabricate the delta-phase ZrH_x pellets to support the development of cladded ZrH_x moderator for advanced reactors.

2 CHALLENGES ASSOCIATED WITH FABRICATING LARGE-SCALE BULK ZIRCONIUM HYDRIDE

The zirconium-hydrogen (Zr-H) binary phase diagram and the pressure-composition-temperature relationship are the two most important pieces of information needed to guide the fabrication of crack-free zirconium hydride. A reliable thermodynamics database has been established. Figure 1 shows the phase diagram for Zr-H system with equilibrium H_2 isobars [9]. The equilibrium hydrogen pressure as a function of temperature and H/Zr ratio is calculated by using Eq. (1), where C is the H/Zr atomic ratio[10].

$$p_{H_2\text{-eq}}\ [\text{MPa}] = \left(\frac{C}{2-C}\right)^2 \exp\left(5.72 + 5.21C - \frac{172\ [\text{kJ mol}^{-1}]}{RT\ [\text{K}]}\right) \quad (1)$$

The zirconium hydrogen solid solution (α and β phase), the δ phase-hydride, and the ε phase-hydride are present in the binary H-Zr system. In the α-phase region, hydrogen atoms reside in the lower energy tetrahedral interstitial sites of the hexagonal close packed (HCP) zirconium lattice (a=0.32333nm, c=0.51523nm). The β phase at high temperature has a body-centered cubic (BCC) crystal structure with a lattice parameter of 0.3614nm. The δ phase-hydride has a face-centered cubic (FCC) crystal structure (a=0.4779nm) with a CaF_2 prototype structure. In the ε phase region, hydrogen atoms occupy all available interstitial sites in the HCP structure of ZrH_2 (a=0.35179nm, c=0.4779nm).

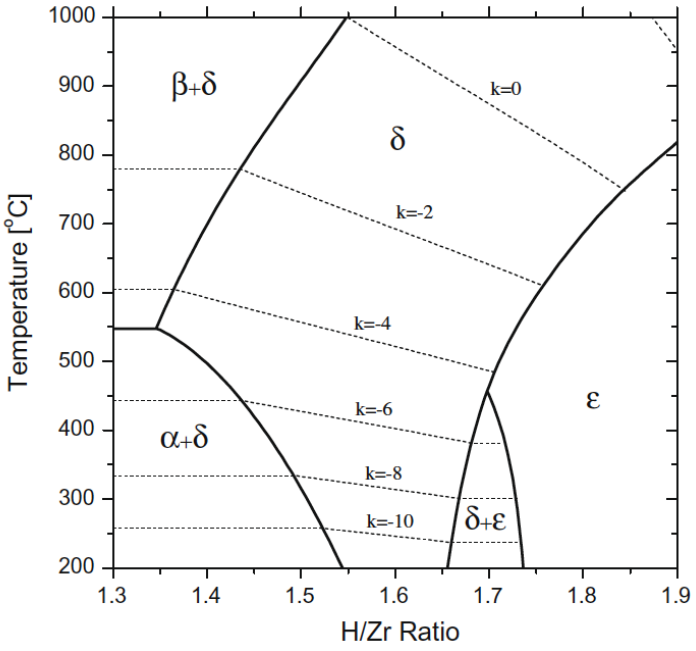

Figure 1. Phase diagram of Zr-H system with equilibrium H_2 isobars labeled as $P_{H2}=10^k$ (MPa).

Hydriding is a rate-controlled exothermic process [11]. The rate limiting process is diffusion of hydrogen inside the solid metal or hydride. Phase transformation of the metal to hydride (or vice versa) is a moving boundary growth process in Zr-H system [12]. However, the interfacial reaction rate is not deemed as rate limiting. The most significant challenge in fabricating massive crack-free bulk metal hydride (or during rapid dehydriding) is that if the hydrogen concentration gradient across the sample body is not managed to a low value, then differential lattice strain persists, leading to significant stress. This stress, coupled with the low fracture toughness of the hydride materials, is the ultimate source of cracking, and it is routinely exploited to produce powder from various metals in the hydride-dehydride process. In this work, finite element analysis was performed using BISON [13] to semi-quantitatively demonstrate the stress distribution in a zirconium sphere of 1 mm in diameter under various hydrogen concentration gradients along the radial direction. The simulation temperature was set to 823K, and it remained constant without considering the exothermic nature of the hydriding process. The swelling of zirconium hydride was assumed to be proportional to the H/Zr atomic ratio. The swelling was 14.3 % at ZrH_2 and 0 for Zr, linearly increasing between these values. The elastic modulus was set to 95 GPa for Zr and 130 GPa for ZrH_2 [14], linearly increasing with hydrogen concentration. The Poisson's ratio was set to a constant value of 0.32 [14]. The densities of zirconium and zirconium hydride were set to 6.49 and 5.56 g/cm^3, respectively [15]. A linear correlation between density and the H/Zr ratio was assumed. Four cases were evaluated: (a) the H/Zr atomic ratio as 0 for radii less than 0.21 mm and 2.0 otherwise; (b) the H/Zr ratio linearly increasing for radii greater than 0.21 mm from 0 to 2.0; (c) the hydrogen concentration following a linear gradient through the radius from 0.01 to 2.0; and (d) the H/Zr ratio linear increasing from 1.90 to 2.0, starting from the radius of 0.

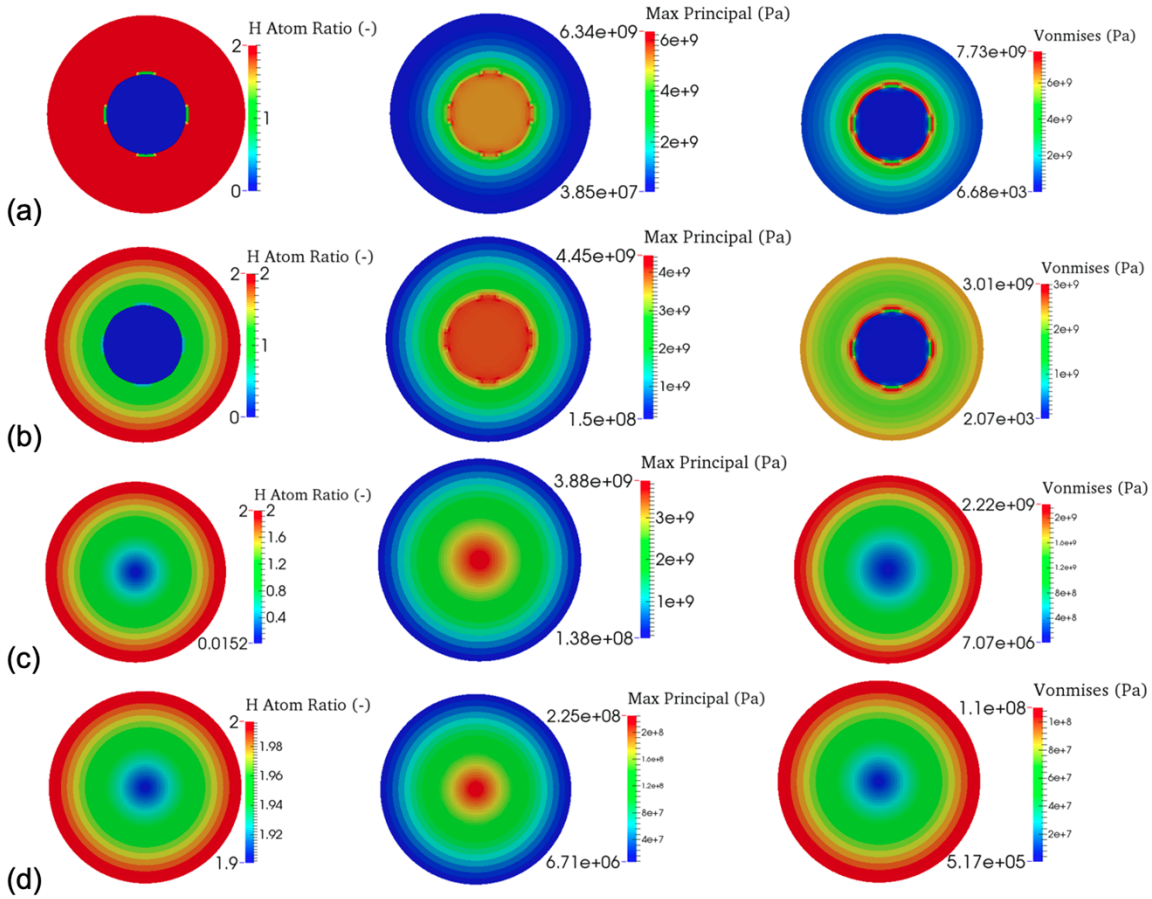

Figure 2. The hydrogen concentration gradient, the maximum principal stress, and the von Mises stress distribution for four distinct H concentration profiles. The H concertation gradients (left) become more gradual and flat moving from scenario (a) to (d), resulting in the lower stresses arising from lattice differential strain (right).

Figure 2 shows the hydrogen concentration gradient, the maximum principal stress (relevant when assessing brittle hydride), and the von Mises stress (relevant for assessing ductile metal) distribution in each case. In the first three simulations, significant stress built up within the spherical sample. Case 1, with the sharpest change in hydrogen concentration, had the highest stress. The zirconium hydride perimeter swells and attempts to pull the zirconium core outward. Thus, the zirconium hydride region was subjected to strong compressive hoop stress but tensile radial stresses, while the zirconium region was subjected to tensile hoop stress and radial stress. The inner zirconium region was equitriaxial, which causes the von Mises stress to be very small in the center. This analysis implies that the cracks could initiate anywhere in the zirconium region or Zr/ZrH_x interface. Figure 3 shows optical micrographs of two cracked ZrH_x samples that were fabricated under conditions that rapidly supplied H into the solid, resulting in a large hydrogen concentration gradient throughout the hydrided work pieces (i.e., the H gas–solid surface flux is much larger than the H diffusive flux in the solid).

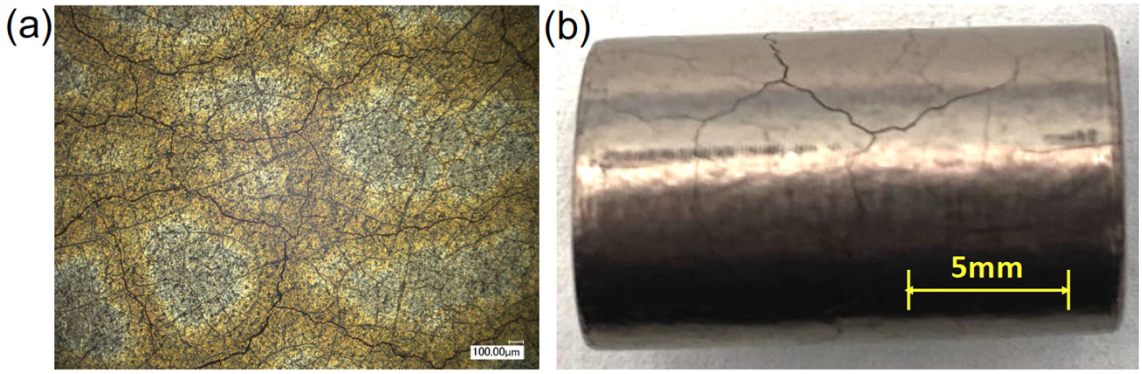

Figure 3. (a) Surface of a cracked zirconium hydride disk and (b) a cracked zirconium hydride rod resulting from the presence of the large hydrogen concentration gradients within the samples during fabrication.

The fourth simulation considered a case with a shallow H concentration gradient in which the center was $ZrH_{1.9}$ and the surface was ZrH_2. This represents a scenario in which H was slowly supplied to the solid, so there was ample time for diffusive flux to flatten the H concentration profile inside the solid. This simulation predicted much smaller stresses. Therefore, crack prevention appears to be clearly a matter of preventing large concentration gradients within the sample. A practical approach is to initiate hydriding at the desired final temperature, and limiting the rate of hydriding at said temperature can be achieved by applying a small hydrogen flow rate. This low flow rate effectively allows more time for hydrogen redistribution (via bulk diffusion process) within the workpiece, and thus avoiding an adverse hydrogen concentration gradient within the sample. Uniformity of retort temperature is generally of primary importance in producing sound massive metal hydrides with uniform hydrogen/metal atom ratios.

3 FABRICATION OF DELTA-PHASE ZIRCONIUM HYDRIDES

A fully programmable hydriding system with continuous hydrogen partial pressure and flow control coordinated with precise temperature control has been designed and constructed at Oak Ridge National Laboratory (ORNL) under the Transformational Challenge Reactor (TCR) Program to fabricate metal hydride. A schematic plot of this system is shown in Figure 4: an ultra-high vacuum system consisting of all metal parts and fittings capable of a vacuum level of 2×10^{-8} torr. The maximum temperature of the 3-zone tube furnace is 1,100°C. An Inconel retort is employed to process the sample. The programmable gas control system was designed to enable flow control coordinated with temperature control. An automatic emergency cut-off system with a safety inert gas purge line and a pressure relief valve was included to ensure safe hydrogen handling.

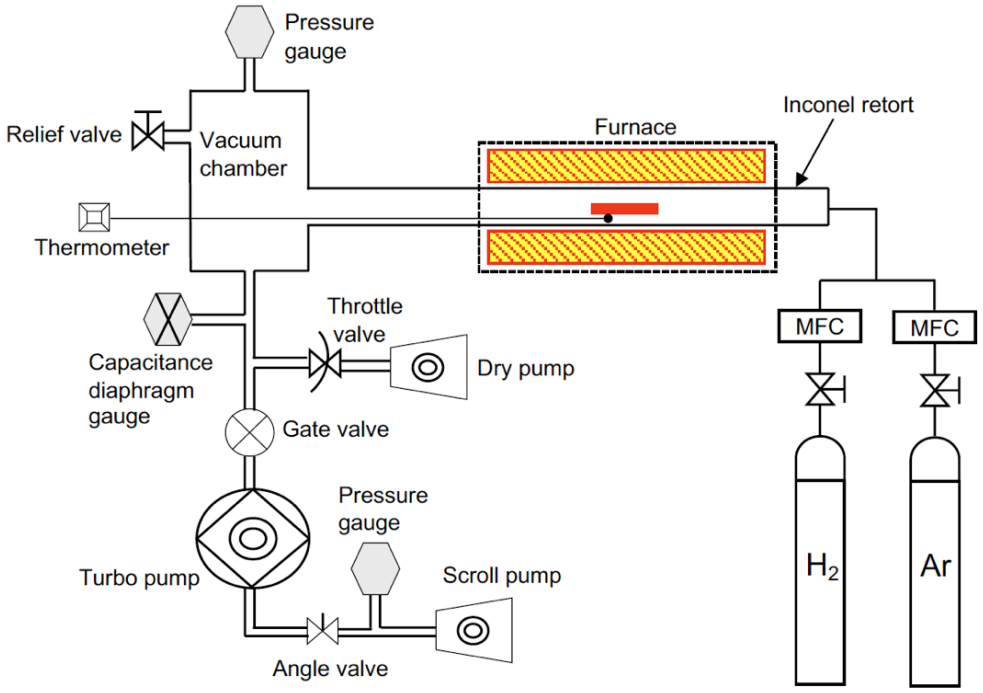

Figure 4. Schematic of the TCR bulk metal hydriding system at ORNL[16].

Instead of introducing a set amount of hydrogen to the retort, ZrH_x is fabricated by carefully matching the retort temperature and the hydrogen partial pressure. The process was initiated with ultra–high-purity zirconium metal—99.9%, purchased from American Elements. The typical hydriding process is designed as follows:

1. Evacuate the retort after loading zirconium samples and purge the sealed system with ultra-high purity Ar gas;
2. Heat the retort to 900°C to degas under vacuum, and then lower the retort temperature to the pre-determined processing temperature;
3. Isolate the retort from the pumping system using the gate valve;
4. Introduce ultra–high-purity hydrogen to the retort at a low flow rate ranging from 5 to 150 standard cubic centimeters per minute (sccm), depending on the surface area of the material to be hydrided;
5. Maintain the hydrogen pressure within the retort to a predetermined value that, together with the processing temperature, determines the H/Zr atomic ratio of the final product, and maintain a close coordination of the throttle valve, the mass flow controller, and the capacitance diaphragm gauge to yield the constant retort pressure;
6. Bring the retort to room temperature following the temperature-pressure isochore line. Precise pressure control corresponding to the retort temperature is achieved using the same instruments during this step.

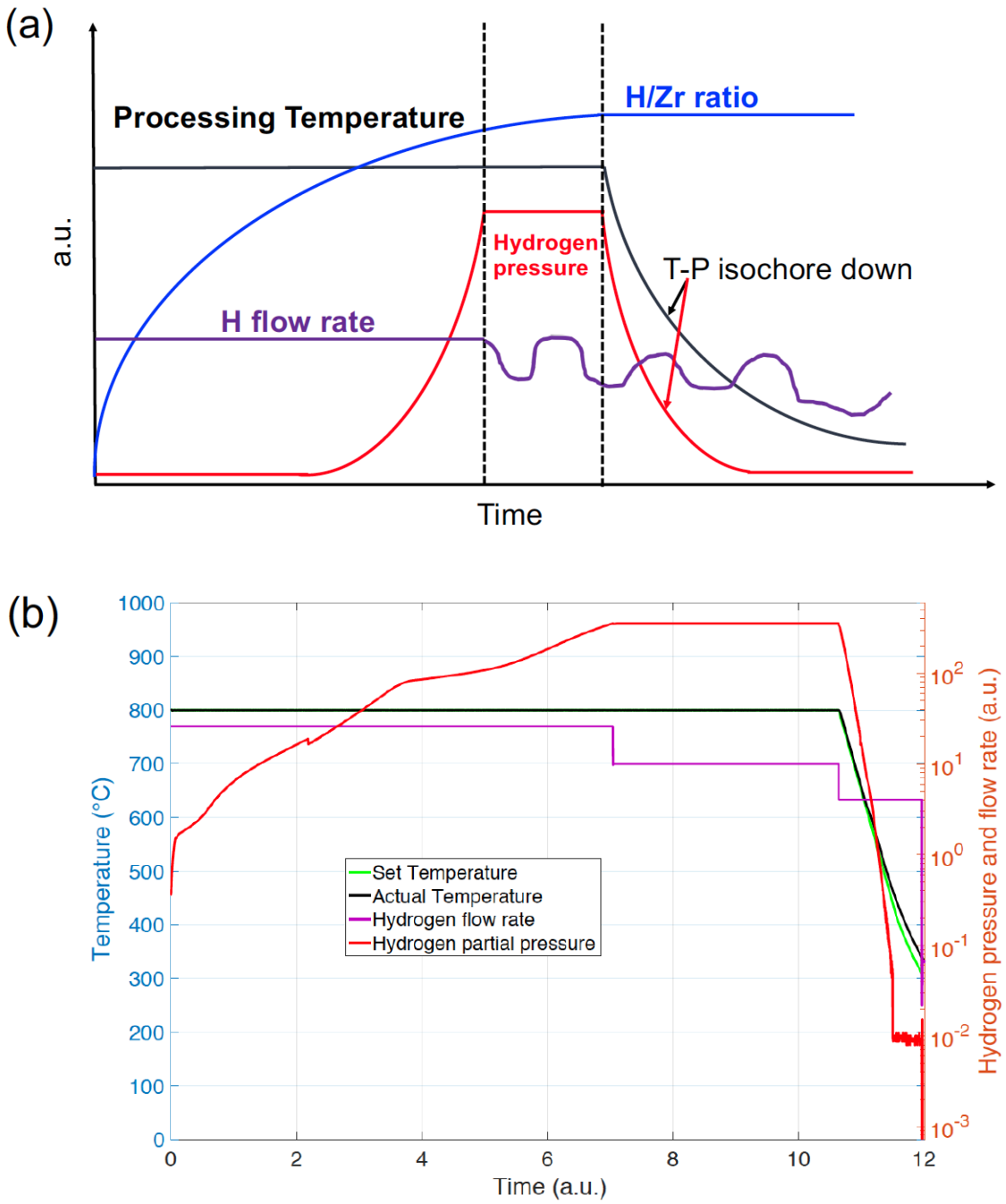

Figure 5. (a) Schematic plot of the evolution of retort temperature, hydrogen partial pressure, hydrogen flow rate, and H/Zr atomic ratio during a desired hydriding process, and (b) the important processing parameters recorded during a typical hydriding process. a.u. refers to arbitrary unit.

The evolution of important parameters during the hydriding process is schematically shown in Figure 5(a). A constant hydrogen flow rate is initially maintained to provide hydrogen supply to the retort. The work piece rapidly absorbs the introduced hydrogen, resulting in a stable vacuum environment in the retort. Then the hydrogen pressure in the retort begins

to increase slowly, indicating the onset of hydride formation. Eventually, the hydrogen pressure reaches a threshold that is predetermined based on the desired H/Zr atomic ratio in the final product and the processing temperature. The hydrogen's partial pressure in the retort will remain constant to enable homogeneous distribution of the hydrogen across the sample. During the cooling process, the temperature-pressure isochore line must be followed to maintain the H/Zr atomic ratio in the final product, which requires the simultaneous controls of temperature and hydrogen partial pressure. An *isochore* is a line of constant composition on a plot of temperature vs. pressure, which has been well established through thermodynamics studies [9]. By following the isochore line, it is possible to maintain the hydrogen concentration in the fabricated ZrH_x without either absorbing hydrogen from or evolving it to the surrounding atmosphere during the furnace cooling process. Figure 5(b) shows the hydrogen partial pressure, the hydrogen flow rate, and the temperatures recorded during a typical hydriding process.

4 CHARACTERIZATION OF AS-FABRICATED ZIRCONIUM HYDRIDE PELLETS

Following the above-mentioned fabrication procedure, we have successfully fabricated delta-phase zirconium hydride pellets through carefully controlling the hydrogen flow rate. Figure 3(a) showed the picture of two long zirconium hydride rods (11 mm in diameter, 105 mm in length) with H/Zr atom ratios of 1.608 and 1.607, respectively. Small ZrH_x pellets (8.3 mm in diameter, 18.9 mm in height) are shown in Figure 3 (b) with H/Zr ratio of ~1.57. The hydrogen content of as-fabricated zirconium hydride samples was determined based on the weight change, which was assumed to be due to the absorption of hydrogen during the hydriding process. The H/Zr atomic ratios of these fabricated hydride correspond to the delta-phase zirconium hydride. Table 1 lists the weight change and the calculated H/Zr atom ratio of 16 ZrH_x pellets.

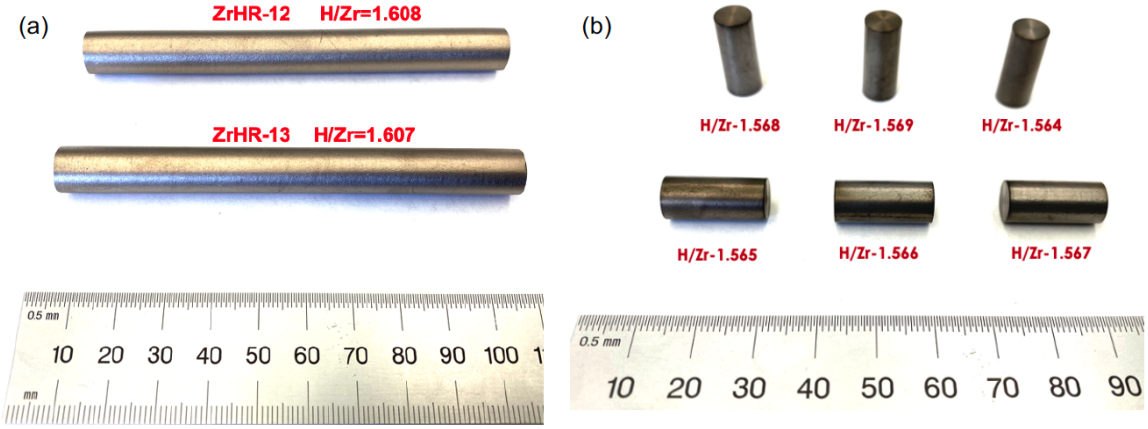

Figure 6. As-fabricated (a) zirconium hydride long rods and (b) pellets.

Table 2. ZrHx fabricated by using the ORNL TCR bulk metal hydriding system

Sample	Weight of starting zirconium metal (g)	Weight of as-fabricated ZrH_x (g)	Absorbed H amount (mol)	H/Zr atom ratio
ZrH-9	7.7179	7.8535	0.1356	1.622
ZrH-10	53.9813	54.8937	0.9124	1.561
ZrH-11	53.7468	54.6790	0.9322	1.601
ZrH-12	53.8231	54.7606	0.9375	1.608
ZrH-13	53.8862	54.8242	0.9380	1.607
ZrH-14	5.6039	5.6991	0.0952	1.568
ZrH-15	5.6052	5.7005	0.0953	1.570
ZrH-16	5.6072	5.7022	0.0950	1.564
ZrH-17	5.6148	5.7100	0.0952	1.566
ZrH-18	5.6072	5.7023	0.0951	1.566
ZrH-19	5.6192	5.7146	0.0954	1.568
ZrH-20	7.5522	7.8873	0.1351	1.609
MITR-1	5.6061	5.7005	0.0944	1.555
MITR-2	5.6203	5.7157	0.0954	1.567
MITR-3	5.6186	5.7156	0.0970	1.594
MITR-4	5.6222	5.7188	0.0966	1.586

X-ray diffraction (XRD) was employed to confirm the phases present in the fabricated hydride samples. Powder samples were made such that material from the center to the surface of the bulk samples was present. When necessary, samples were also mixed with NIST 640D Si powder as an internal standard during pattern refinement. Powders were dispersed onto flat low-background holders with isopropanol. High-resolution 2θ-θ diffraction patterns were obtained using a Bruker D2 Phaser benchtop X-ray diffractometer of 0.30 kW with Cu Kα radiation. XRD analysis of five as-fabricated zirconium hydride specimens (Figure 5) indicated that single delta-phase zirconium hydride was successfully fabricated in all measured samples.

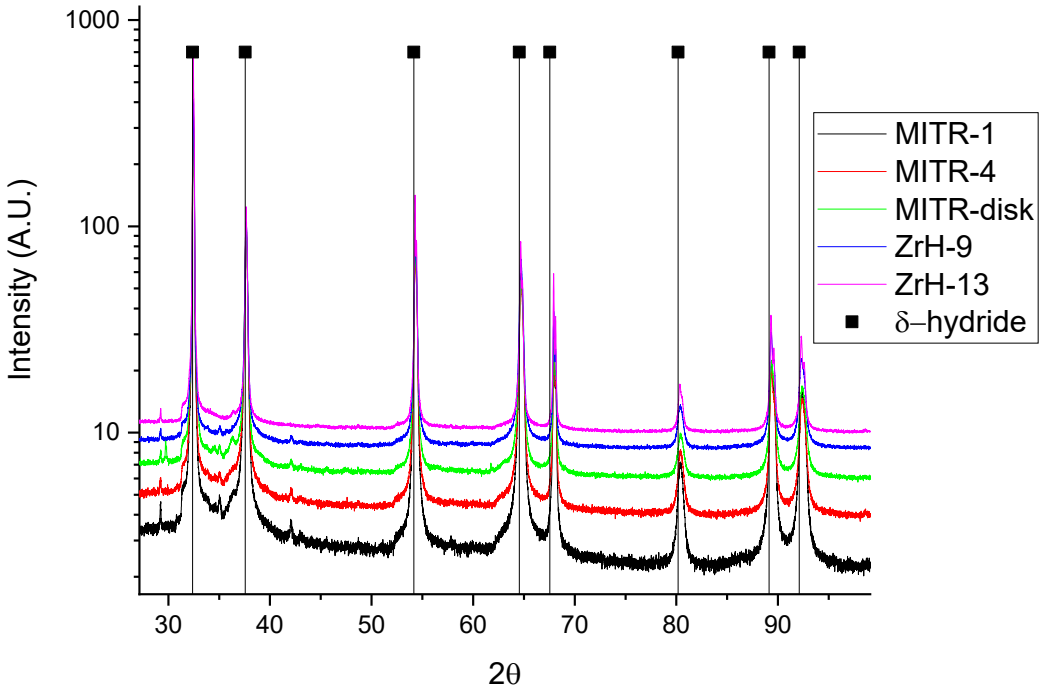

Figure 7. XRD pattern of as-fabricated zirconium hydride samples with expected delta-phase zirconium hydride peak locations marked.

X-ray computed tomography (XCT) was employed to investigate any possible cracking of the fabricated zirconium hydrides. XCT measurement were conducted using a Zeiss Xradia microscope operating at 140kV/71µA. 1600 X-ray radiographs were collected for each specimen with a 7 s dwell time. Volume reconstructions were performed in Zeiss Scout and Scan and corrected for any sample offset and beam hardening effects. The XCT images (Figure 8a) showed that surface cracks penetrating ~550μm were found in ZrH-19. Similar surface conditions were also found in the samples of ZrH-12 and ZrH-16. There is no internal cracking identified in all fabricated hydride samples. It is noted that all fabricated disk samples (6mm in diameter and 1mm in thickness) are all crack-free, as shown in Figure 8b.

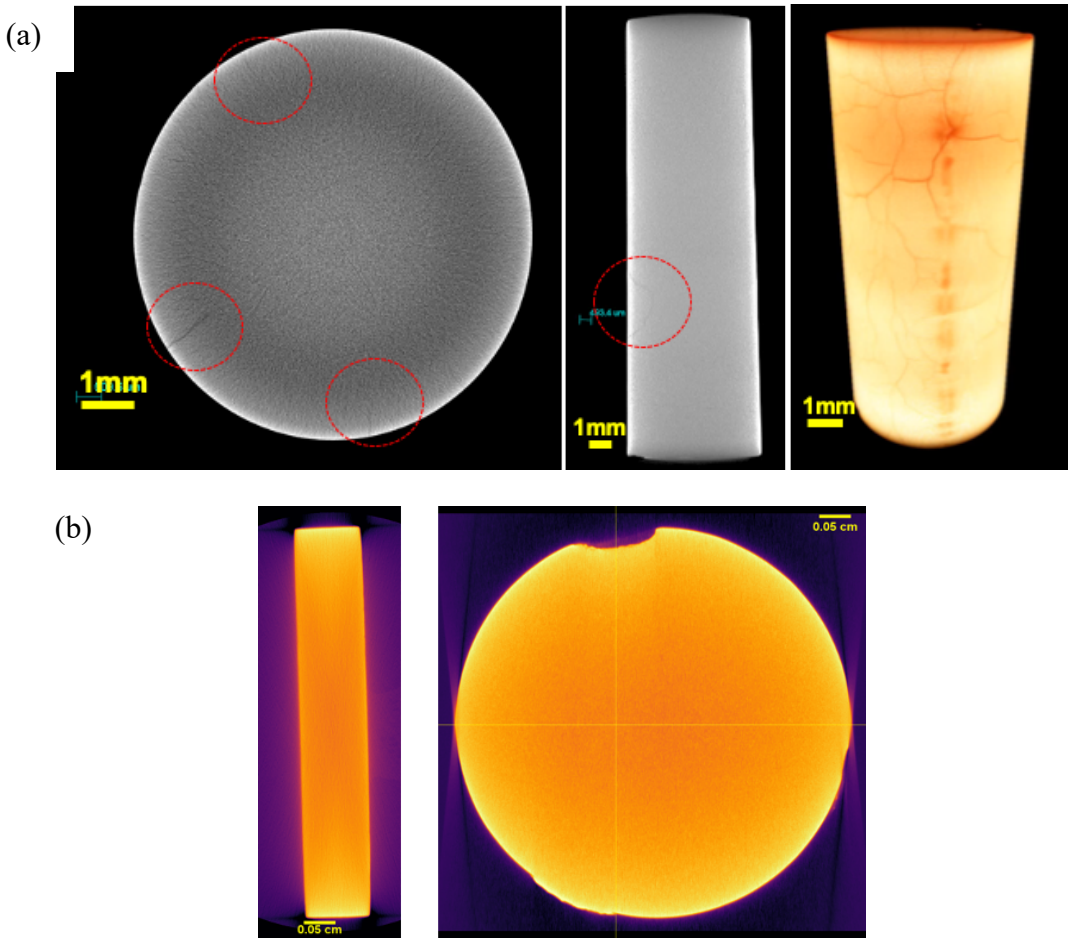

Figure 8. XCT images of (a) ZrH-19 rod (H/Zr=1.568, 8.3 mm in diameter, 18.9 mm in height) and (b) a $ZrH_{1.58}$ disk

We further reduced the hydrogen flow rate from 25 sccm to 15 sccm during the hydriding process of the zirconium pellets, which gives rise to the crack free hydride pellets (10mm in diameter, 15mm in height). Figure 9 showed a snapshot of cross section of ZrH-20 from the XCT reconstruction. No cracking was observable. It is noted that this XCT measurement was conducted using a ZEISS Metrotom M800 (200 kV/14 W power) at ORNL. A single scan (1 hour) was conducted to evaluate the whole volume of the specimen. The resolution varies from 9~13 voxel size.

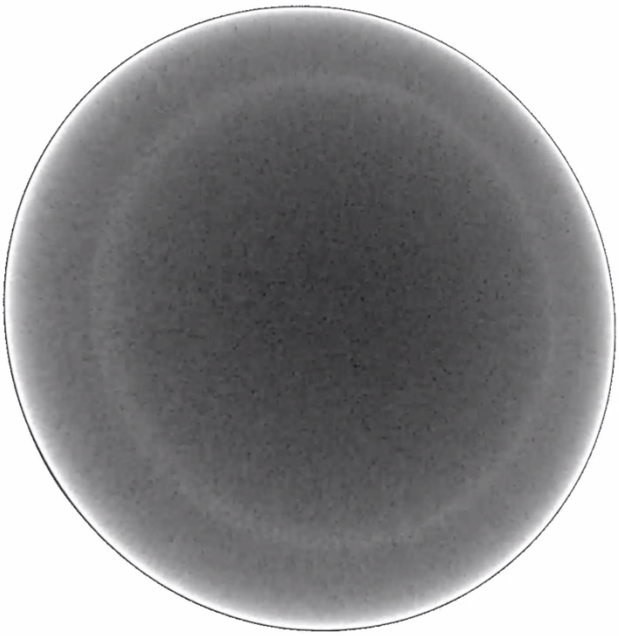

Figure 9. XCT image of the cross section of ZrH-20 (H/Zr=1.609)

5 SUMMARY

In this report, we summarized our effort to fabricate bulk delta-phase zirconium hydride. The challenges in fabricating crack-free zirconium hydride are discussed. A fully programmable hydriding system with continuous hydrogen partial pressure and flow control was employed to facilitate processing of massive monolithic metal hydride specimens. The working principle of the hydriding system was introduced. Characterization of the produced zirconium hydride specimens included X-ray powder diffraction to identify the present phases and X-ray Computed Tomography to visualize internal microstructure (including cracks). Delta-phase zirconium hydride pellets have been successfully fabricated. Reducing the hydrogen flowing rate leads to the fabrication of crack-free zirconium hydride pellets. These hydride pellets will be further used for the cladding development, which will be reported in the next milestone report.

6 REFERENCES

1. Edwards, P.P., V.L. Kuznetsov, and W.I. David, *Hydrogen energy.* Philos Trans A Math Phys Eng Sci, 2007. **365**(1853): p. 1043-56.
2. Sakintuna, B., F. Lamaridarkrim, and M. Hirscher, *Metal hydride materials for solid hydrogen storage: A review☆.* International Journal of Hydrogen Energy, 2007. **32**(9): p. 1121-1140.
3. Van Houten, R., *Selected Engineering And Fabrication Aspects Of Nuclear Metal Hydrides (Li, Ti, Zr, And Y).* Nuclear Engineering and Design, 1974. **31**: p. 434-448.
4. Davies, N. and R. Forrester, *Effects of irradiation on hydrided zirconium-uranium alloy NAA 120-4 experiment*. 1970, Atomics International Div.: Canoga Park, CA.

5. Simnad, M., *The U-ZrHx alloy: Its properties and use in TRIGA fuel.* Nuclear Engineering and Design, 1981. **64**(3): p. 403-422.
6. Haslett, R., *Space Nuclear Thermal Propulsion Program*. 1995, Grumman Aerospace Corp.: Bethpage, NY.
7. Van Houten, R., *Massive Metal Hydride Structures And Methods For Their Preparation.* US3720752, 1973.
8. Van Houten, R., *Hydriding Process.* US3720751, 1973.
9. Terrani, K.A., et al., *The kinetics of hydrogen desorption from and adsorption on zirconium hydride.* Journal of Nuclear Materials, 2010. **397**(1-3): p. 61-68.
10. Wang, W.-E. and D.R. Olander, *Thermodinamycs of Zr-H System.* J. Am. Ceram. Soc., 1995. **78**: p. 3323-28.
11. Mueller, W.M., J.P. Blackledge, and G.G. Libowitz, *Metal Hydrides.* Academic Press New York and London, 1968.
12. Hu, X., K.A. Terrani, and B.D. Wirth, *Hydrogen desorption kinetics from zirconium hydride and zirconium metal in vacuum.* Journal of Nuclear Materials, 2014. **448**(1-3): p. 87-95.
13. Williamson, R.L., et al., *Multidimensional multiphysics simulation of nuclear fuel behavior.* Journal of Nuclear Materials, 2012. **423**(1-3): p. 149-163.
14. Yamanaka, S., et al., *Thermal and mechanical properties of zirconium hydride.* Journal of Alloys and Compounds, 1999. **293-295**(20): p. 23-29.
15. Ito, M., *Studies on Physical Properties of Metal Hydrides and Hydrogen Behavior in Zr Alloys.* Osaka University, 2008. **PhD Thesis**.
16. Hu, X., et al., *Fabrication of yttrium hydride for high-temperature moderator application.* Journal of Nuclear Materials, 2020. **539**: p. 152335.